









Perfluorocycloparaphenylenes

Hiroki Shudo¹, Motonobu Kuwayama ^{2,3}, Masafumi Shimasaki ⁴, Taishi Nishihara ⁴, Youhei Takeda ⁵, Nobuhiko Mitoma ⁶, Takuya Kuwabara ^{1,2,3}, Akiko Yagi^{1,3}, Yasutomo Segawa ^{1,2,7,8}✉ & Kenichiro Itami ^{1,2,3}✉

Perfluorinated aromatic compounds, the so-called perfluoroarenes, are widely used in materials science owing to their high electron affinity and characteristic intermolecular interactions. However, methods to synthesize highly strained perfluoroarenes are limited, which greatly limits their structural diversity. Herein, we report the synthesis and isolation of perfluorocycloparaphenylenes (PFCPPs) as a class of ring-shaped perfluoroarenes. Using macrocyclic nickel complexes, we succeeded in synthesizing PF[*n*]CPPs (*n* = 10, 12, 14, 16) in one-pot without noble metals. The molecular structures of PF[*n*]CPPs (*n* = 10, 12, 14) were determined by X-ray crystallography to confirm their tubular alignment. Photophysical and electrochemical measurements revealed that PF[*n*]CPPs (*n* = 10, 12, 14) exhibited wide HOMO–LUMO gaps, high reduction potentials, and strong phosphorescence at low temperature. PFCPPs are not only useful as electron-accepting organic materials but can also be used for accelerating the creation of topologically unique molecular nanocarbon materials.

¹Graduate School of Science, Nagoya University, Nagoya 464-8602, Japan. ²JST, ERATO, Itami Molecular Nanocarbon Project, Nagoya University, Nagoya 464-8602, Japan. ³Institute of Transformative Bio-Molecules (WPI-ITbM) Nagoya University, Nagoya 464-8602, Japan. ⁴Institute of Advanced Energy, Kyoto University, Kyoto 611-0011, Japan. ⁵Department of Applied Chemistry, Graduate School of Engineering, Osaka University, Yamadaoka 2-1, Suita, Osaka 565-0871, Japan. ⁶RIKEN Center for Emergent Matter Science, Wako 351-0198, Japan. ⁷Institute for Molecular Science, Myodaiji, Okazaki 444-8787, Japan. ⁸Department of Structural Molecular Science, SOKENDAI (The Graduate University for Advanced Studies), Myodaiji, Okazaki 444-8787, Japan. ✉email: segawa@ims.ac.jp; itami@chem.nagoya-u.ac.jp

Organic fluorine compounds have found widespread applications in pharmaceutical, agricultural, and materials science^{1–5}. The introduction of fluorine into organic molecules often strongly affects their properties, including their polarity, solubility, and lipophilicity. Among many organic fluorine-containing compounds, fluorinated arenes are used as semiconductors, light-emitting materials, and liquid crystals⁶. Owing to its negative inductive effect, the incorporation of fluorine into materials leads to a decrease in orbital energy. As such, it is important to develop synthetic methods that provide access to aromatic molecules containing many C–F bonds^{7–9}, and the extreme targets of the research field are aromatic molecules wherein all hydrogen atoms are replaced with fluorine atoms, i.e., perfluoroarenes^{10–14}. However, methods to synthesize strained perfluoroarenes remain very limited. It is known that various fluorinated fullerenes (Fig. 1a, top left) can be obtained from the addition of fluorine to the unsaturated bonds of fullerenes, but these are virtually the only examples of highly strained perfluoroarenes¹⁵. Although Suzuki and co-workers have shown that perfluororubrene (Fig. 1a, top right) possesses a twisted

structure with a slight strain¹⁶, a method to apply more strain to perfluoroarenes has not yet been reported.

Perfluorocycloparaphenylenes (PFCPPs) are a class of highly strained ring-shaped perfluoroarenes (Fig. 1a, bottom) in which all hydrogen atoms of the corresponding cycloparaphenylenes (CPPs)^{17–19} are replaced with fluorine atoms. This replacement of hydrogen with fluorine can be expected to result in a significant change of the structural and electronic properties of the PFCPPs²⁰. Two major methods for the synthesis of CPPs have been reported: (i) converting C₆ units, such as cyclohexane and cyclohexadiene, of macrocyclic precursors into benzene rings^{21,22}, and (ii) reductive elimination from macrocyclic metal–arene complexes (metal = Pt, Ni, Au)^{23–25}. However, even partially fluorinated CPPs (F₈[6]CPP, F₁₂[9]CPP, F₈[12]CPP, F₈[10]CPP, F₈[12]CPP) synthesized by the groups of Yamago and Jasti^{26–28} require multiple steps (method (i), Fig. 1b), and there has no successful synthesis of CPP derivatives from *ortho*-functionalized aryl groups by the Pt method^{17–19}. We hypothesized that PFCPPs can be obtained in one-pot based on method (ii). Considering that the reductive elimination of perfluorobiphenyl occurs from the stable (2,2′-bipyridyl)Ni(C₆F₅)₂ complex promoted by acids or oxidants^{29,30}, Ni might be a suitable metal for the construction of macrocyclic precursors for PFCPPs (Fig. 1c).

Herein, we report the synthesis and isolation of PFCPPs. Using macrocyclic nickel complexes, PF[*n*]CPPs (*n* = 10, 12, 14, 16) were obtained in one-pot without using noble metals. The molecular structures of PF[*n*]CPPs (*n* = 10, 12, 14) were determined by X-ray crystallography to confirm their structures and tubular alignment. PF[*n*]CPPs (*n* = 10, 12, 14) exhibited wide HOMO–LUMO gaps, high reduction potentials, and strong phosphorescence at low temperature.

Results and discussion

Synthesis of PFCPPs. Our synthetic route to PFCPPs is outlined in Fig. 2. Starting from 2,3,5,6,2′,3′,5′,6′-octafluorobiphenyl (**1**), deprotonation by lithium diisopropylamide (LDA) and subsequent transmetalation to Ni(dnbpy)Br₂ (dnbpy = 4,4′-di-*n*-nonyl-2,2′-bipyridyl) produced a mixture of macrocyclic complex **2**. After evaporation of the solvent and replacing it with *m*-xylene, 2,3-dichloro-5,6-dicyano-*p*-benzoquinone (DDQ) was added and the resulting mixture was stirred at 130 °C for 5 h to promote the reductive elimination of aryl–aryl bonds from Ni. By the purification with silica gel chromatography and preparative recycle GPC, PF[*n*]CPPs (*n* = 10, 12, 14, 16) were obtained in 4.7%, 2.2%, 1.2%, and 0.7% yield, respectively. These PF[*n*]CPPs are highly strained perfluoroarenes, as evident from their high strain energies of 60.2 (*n* = 10), 49.9 (*n* = 12), 42.6 (*n* = 14), and 37.2 kcal·mol^{−1} (*n* = 16) estimated by density-functional theory (DFT) calculations (for details, see Supplementary Fig. 10 in Supplementary Information (SI)). Considering that PF[*n*]CPPs were not obtained when 2,2′-bipyridyl or 4,4′-di-*t*-butyl-2,2′-bipyridyl was used, the *n*-nonyl groups of the dnbpy ligand should be crucial for preventing the precipitation of intermediates. For each PF[*n*]CPP (*n* = 10, 12, 14, 16), one singlet signal was observed in the ¹⁹F NMR spectra at −138.25 (*n* = 10), −138.50 (*n* = 12), −138.64 (*n* = 14), and −138.84 ppm (*n* = 16), where the trend to shift resonances to lower magnetic field with increasing ring size is similar to the case of ¹H NMR chemical shifts of [*n*]CPPs¹⁷. Two singlet signals observed in the ¹³C{¹⁹F} NMR spectra also agreed with the high-symmetric structures of PFCPPs. The corresponding high-resolution mass spectra were recorded using the negative mode of the LDI-TOF MS (laser desorption/ionization time-of-flight mass spectrometry) technique. IR and Raman spectra of PFCPPs are in good agreement with the calculated spectra by B3LYP/6-31G(d) level of theory

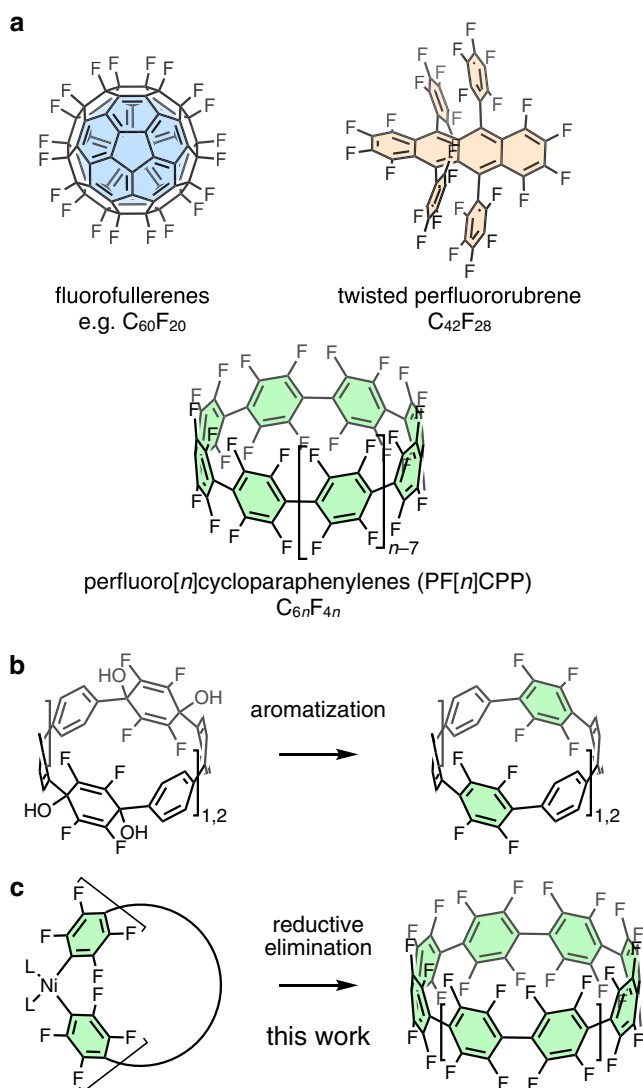


Fig. 1 Fluorocarbon molecules. **a** Structures of fluorofullerenes, perfluororubrene, perfluorocoronullene (top), and perfluorocycloparaphenylenes (PFCPPs) (bottom). **b** A synthetic scheme of previously reported partially fluorinated CPPs. **c** The synthetic strategy for PFCPPs (this work).

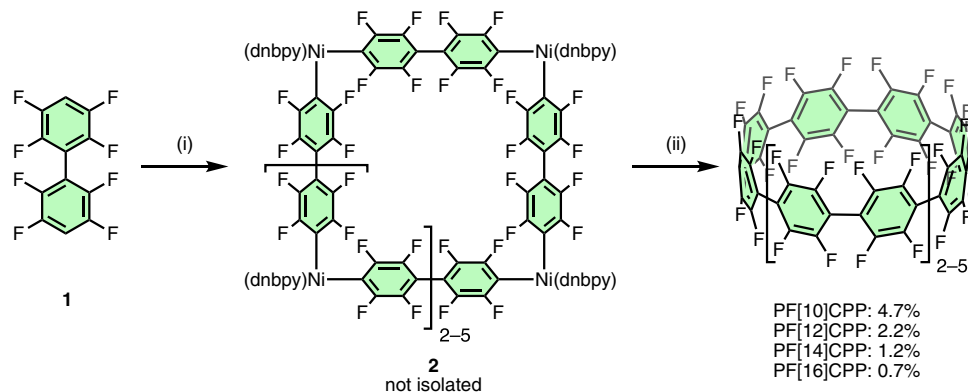


Fig. 2 Synthesis of PFCPPs. Reaction conditions: (i) LDA, Ni(dnbpy)Br₂, THF, -78 °C, 30 min; (ii) DDQ, *m*-xylene, 130 °C, 5 h. LDA = lithium diisopropylamide; dnbpy = 4,4'-di-*n*-nonyl-2,2'-bipyridyl; DDQ = 2,3-dichloro-5,6-dicyano-*p*-benzoquinone.

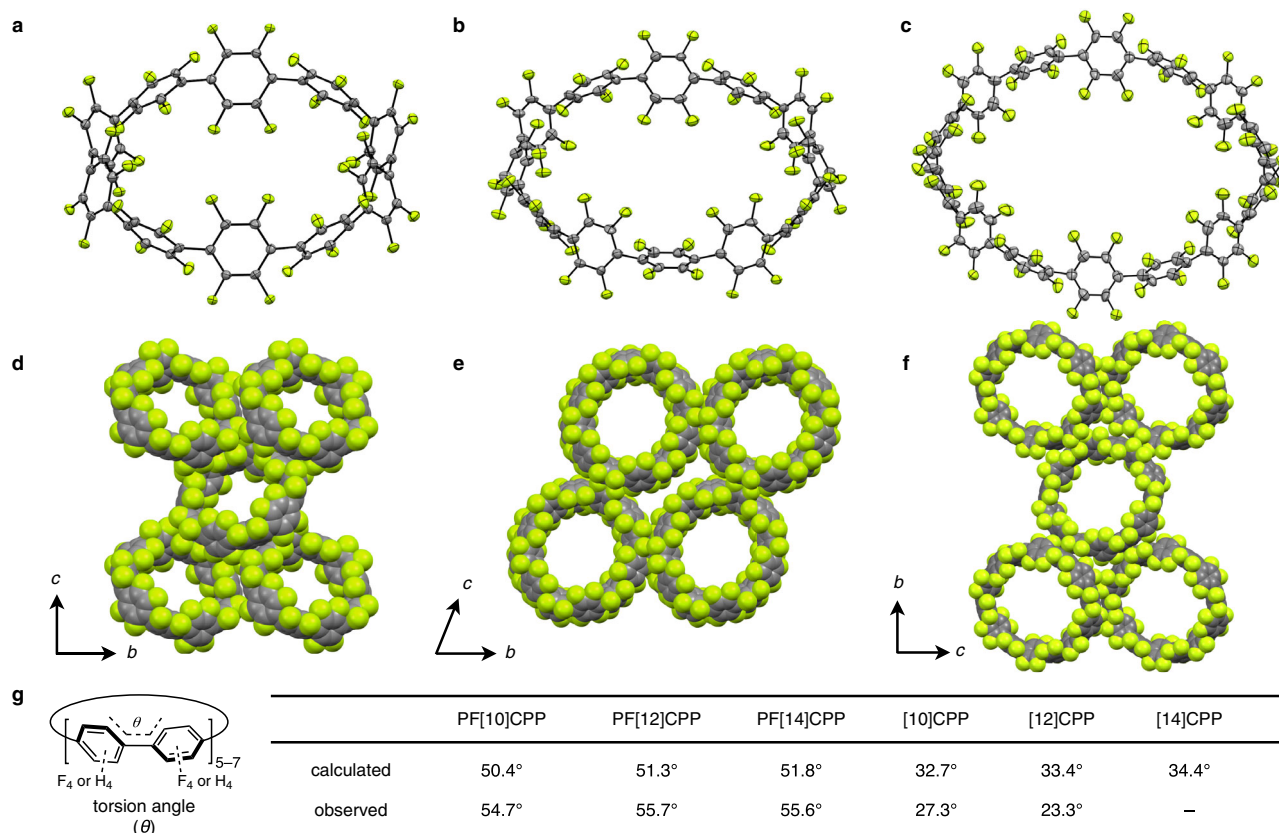


Fig. 3 X-ray crystal structures of PF[n]CPPs ($n = 10, 12, 14$). **a, b, c** Structures of PF[10]CPP (**a**), PF[12]CPP (**b**), and PF[14]CPP (**c**) with thermal ellipsoids at 50% probability. Solvent molecules are omitted for clarity. **d, e, f** Packing structures of PF[10]CPP (**d**), PF[12]CPP (**e**) and PF[14]CPP (**f**); gray: carbon; green: fluorine. Solvent molecules are omitted for clarity. **g** The dihedral angles (θ) around the C-C single bonds of PFCPPs and corresponding CPPs^{31, 32}. Calculations were performed at the B3LYP/6-31G(d) level of theory. Dihedral angles obtained from X-ray crystallography are averaged.

(see Supplementary Fig. 7). Thus, these compounds were identified based on spectral measurements.

Structures of PFCPPs. The structures of PF[n]CPPs ($n = 10, 12, 14$) were successfully determined by X-ray crystallography. Single crystals of PF[10]CPP, PF[12]CPP, and PF[14]CPP were obtained from THF, hexafluorobenzene/*n*-hexane, and chloroform/*n*-pentane solutions, respectively. As shown in Fig. 3a–c, perfluoroarene structures with CPP skeletons (F₄₀[10]CPP, F₄₈[12]CPP, F₅₆[14]CPP) were unambiguously confirmed. For PF[10]CPP, THF used for recrystallization is contained within the ring, despite the fact that these molecules are strongly disordered,

whereas PF[12]CPP contains four molecules of hexafluorobenzene inside and outside the rings. The crystal packing of these PFCPPs is shown in Fig. 3d–f. In PFCPPs, the ring cavities are aligned along the *a*-axis. This result stands in contrast to the behavior of [n]CPPs of the same size ($n = 10, 12$), which show herringbone-like packing^{31,32}, indicating that the influence of fluorine atoms on the molecular alignment in crystal state is significant. Similar tubular packing was also found for partially fluorinated CPPs^{26–28}. The torsion angles between pairs of benzene rings are summarized in Fig. 3g. The averaged dihedral angles observed in X-ray crystallography (PF[10]CPP: 54.7°; PF[12]CPP: 55.7°; PF[14]CPP: 55.6°) and those obtained from

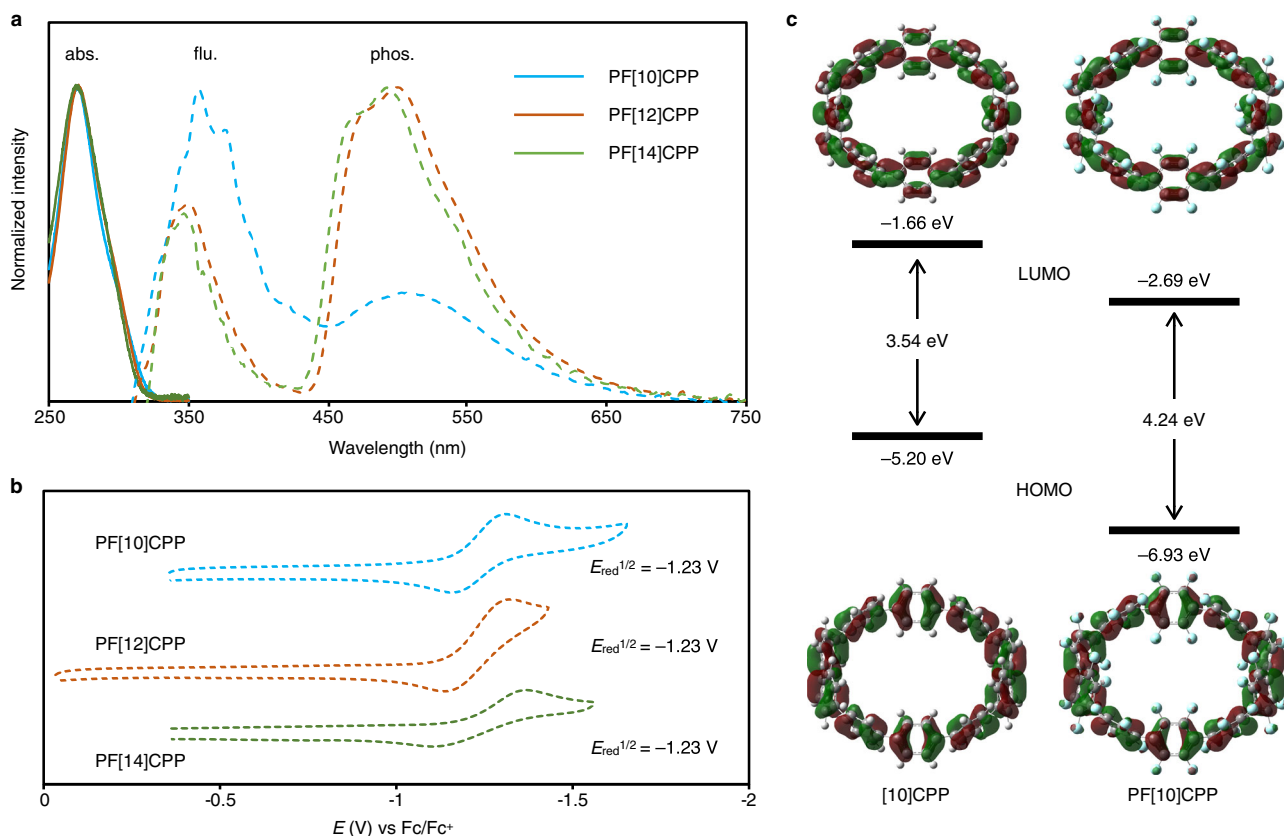


Fig. 4 Photophysical properties of PF[n]CPPs ($n = 10, 12, 14$). **a** UV-Vis absorption spectra of dichloromethane solutions of PFCPPs at room temperature (solid lines), and photoluminescence spectra of PFCPPs in ethanol grass at 77 K upon excitation at 270 nm (dashed lines); blue: PF[10]CPP; red: PF[12]CPP; green: PF[14]CPP. **b** Cyclic voltammograms of PFCPPs in acetonitrile (supporting electrolyte: $[n\text{-Bu}_4\text{N}][\text{PF}_6]$; scan rate: 0.1 V s^{-1}). **c** Frontier molecular orbitals (isovalue: 0.02) and their energies (eV) of [10]CPP and PF[10]CPP calculated by B3LYP/6-31G(d) level of theory. Fc ferrocene.

DFT optimizations at the B3LYP/6-31G(d) level of theory (PF[10]CPP: 50.4° ; PF[12]CPP: 51.3° ; PF[14]CPP: 51.8°) are higher than those of [10]- and [12]CPP (calculated: $\sim 33^\circ$; observed: $23\text{--}27^\circ$)^{31–33}, which is most likely caused by the steric repulsion between fluorine atoms. The interaction between PF[10]CPP and fullerene C_{60} in deuterated chloroform solution was observed (Supplementary Fig. 14)^{34–36}, while the stoichiometry of supramolecular complexes could not be determined by titration experiment because of low solubility of [10]PFCPP and its C_{60} complex.

Electronic properties of PFCPPs. In order to investigate the effect of C–F bonds on the π -electrons in PFCPPs, optical and electrochemical measurements as well as DFT calculations were carried out. The PFCPPs showed absorption in the UV region with absorption peaks at 270 nm (Fig. 4a), which is hypsochromically shifted compared to those of the corresponding CPPs ([10]CPP: 340 nm; [12]CPP: 338 nm; [14]CPP: 338 nm, See Supplementary Fig. 9)^{33,37}. While no obvious fluorescence was detected ($\Phi < 0.01$) at room temperature, bright phosphorescence was observed at low temperature ($\leq 150 \text{ K}$). As shown in Fig. 4a, the PFCPPs in ethanol grass exhibited phosphorescence with peak tops at 507 nm (PF[10]CPP), 500 nm (PF[12]CPP), and 492 nm (PF[14]CPP) at 77 K. The phosphorescence quantum yields (Φ) in ethanol grass at 77 K were 0.21 (PF[10]CPP), 0.62 (PF[12]CPP), and 0.38 (PF[14]CPP). The long lifetimes (τ) of 2.0 s (PF[10]CPP), 0.6 s (PF[12]CPP) and 0.7 s (PF[14]CPP) were also confirmed as the dispersed solid in poly(methyl methacrylate) (for details, see Supplementary Fig. 4 in SI). These photoluminescence properties clearly indicate that intersystem crossing

occurs much more quickly compared to CPPs, which exhibit high-fluorescence quantum yields at room temperature ([10]CPP: 0.46–0.65; [12]CPP: 0.66–0.89, [14]CPP: 0.89)^{33,37}.

Next, cyclic voltammograms were recorded (Fig. 4b). In acetonitrile, all PFCPPs showed a reduction potential (-1.23 V vs ferrocene(II)/ferrocenium(III)) higher than those of previously reported CPPs (e.g., [9]CPP: -2.45 V) and partially fluorinated CPPs (e.g., F_{12} [9]CPP: -2.06 V), indicating that the perfluorination increases the electron affinity of CPPs^{26–28}. Figure 4c shows the HOMO and LUMO of PF[10]CPP with their energies calculated at B3LYP/6-31G(d) level of theory (for details on PF[n]CPPs ($n = 12, 14, 16$), see Supplementary Fig. 9 in SI). While the shape and distribution of each frontier molecular orbital of PF[10]CPP are almost identical to that of [10]CPP, the HOMO–LUMO gap is wider (PF[10]CPP: 4.24 eV) than that of [10]CPP (3.54 eV)³³, which is in line with the hypsochromic shift of the absorption spectra.

In summary, we have synthesized and isolated PF[n]CPPs ($n = 10, 12, 14, 16$), which represent highly strained perfluorocarbon molecules. The synthesis of these PFCPPs was accomplished in a one-pot fashion via deprotonation of octafluorobiphenyl, transmetalation to $\text{Ni}(\text{dnbpy})\text{Br}_2$, and oxidant-promoted reductive elimination. The high solubility of intermediates enhanced by the n -nonyl groups of dnbpy might be the key to the success of this concise synthesis. PF[n]CPPs ($n = 10, 12, 14, 16$) were identified by spectroscopic analysis (^{19}F NMR and LDI-TOF MS, IR, Raman), and the solid-state structures of PF[10]CPP, PF[12]CPP, and PF[14]CPP were unambiguously determined by X-ray crystallography. In the crystal structure, the PFCPPs exhibit a tubular shape, and the ring

cavities are connected one-dimensionally. The dihedral angles between pairs of benzene rings in the PFCPPs are larger than those of the corresponding CPPs due to the steric repulsion between fluorine atoms. Optical and electrochemical measurements revealed wide HOMO–LUMO gaps and high reduction potential for PF[*n*] CPPs (*n* = 10, 12, 14), which also show strong phosphorescence at low temperature. This noble metal-free one-pot synthesis of PFCPPs represents a huge breakthrough in fluorocarbon chemistry. Apart from the obvious interesting electronic features of strained PFCPPs, it should also be possible to create highly strained molecular nanocarbon materials by further converting the reactive C–F bonds of PFCPPs. PFCPPs are not only attractive as electron-deficient aromatic materials but are also potentially applicable to further transformations for the creation of highly strained and topologically unique molecular nanocarbon materials³⁸.

Methods

Synthesis of PF[*n*]CPPs (*n* = 10, 12, 14, 16). To a 200-mL two-necked round-bottomed flask containing a magnetic stirring bar and filled by argon gas were added 2,3,5,6,2',3',5',6'-octafluorobiphenyl (**1**) (1.00 g, 3.35 mmol), Ni(dnbpy)Br₂ (2.10 g, 3.35 mmol), and dry THF (67 mL). The 2.0 M solution of lithium diisopropylamide (LDA) in THF (6.75 mL) was added to the flask at –78 °C. After the reaction mixture was stirred for 30 min, volatile solvents were evaporated in vacuo. The flask was filled by argon gas, and 2,3-dichloro-5,6-dicyano-*p*-benzoquinone (DDQ, 3.81 g, 16.8 mmol) and degassed *m*-xylene (100 mL) were added to the flask. The reaction mixture was stirred at 130 °C for 5 h. After cooling the reaction mixture to room temperature, the reaction mixture was filtrated through Celite® with chloroform (1.0 L), and the resulting filtrate was evaporated in vacuo. The crude product was purified by silica gel column chromatography (eluent: hexane/chloroform = 100:1 to 1:1) and then gel permeation chromatography (GPC; the crude solid (ca.100 mg) was dissolved in 120 mL chloroform, filtered with a Hydrophilic PTFE 0.45 µm Membrane filter (Millex-LCR 13 mm), and each 30 mL of resulting solution was injected to the GPC. Fractions were collected at the fourth cycle (see Supplementary Fig. 1.) to afford PF[*n*]CPPs (*n* = 10: 47.3 mg, 4.7%; *n* = 12: 22.3 mg, 2.2%; *n* = 14, 12.1 mg, 1.2%; *n* = 16: 6.7 mg, 0.7%) as a white solid.

Data availability

Materials and methods, experimental procedures, photophysical studies, and NMR spectra are available in the Supplementary Information. Raw data corresponding to UV–Vis adsorption spectra (Fig. 4a) and Cyclic voltammograms (Fig. 4b) can be found in Supplementary Data File 1 and Supplementary Data 2, respectively. Crystallographic data for the structures reported in this article have been deposited at the Cambridge Crystallographic Data Centre under deposition numbers CCDC 2057897 (PF[10]CPP), 2057898 (PF[12]CPP), and 2133188 (PF[14]CPP). Copies of the data can be obtained free of charge via <https://www.ccdc.cam.ac.uk/structures/>.

Received: 7 March 2022; Accepted: 16 June 2022;

Published online: 28 June 2022

References

- Lemal, D. M. Perspective on fluorocarbon chemistry. *J. Org. Chem.* **69**, 1–11 (2004).
- Politanskaya, L. V. et al. Organofluorine chemistry: promising growth areas and challenges. *Russ. Chem. Rev.* **88**, 425–569 (2019).
- Klaus, M., Christoph, F. & François, D. Fluorine in pharmaceuticals: looking beyond intuition. *Science* **317**, 1881–1886 (2007).
- Purser, S., Moore, P. R., Swallow, S. & Gouverneur, V. Fluorine in medicinal chemistry. *Chem. Soc. Rev.* **37**, 320–330 (2008).
- Brzhezinskaya, M. M. et al. Specific features of the electronic structure of fluorinated multiwalled carbon nanotubes in the near-surface region. *Phys. Solid State* **51**, 1961–1971 (2009).
- Tang, M. L. & Bao, Z. Halogenated materials as organic semiconductors. *Chem. Mater.* **23**, 446–455 (2011).
- Birchall, J. M. & Flowers, W. T. In *Fluorocarbon and Related Chemistry* (eds. Banks, R. E. & Barlow, M. G.) Vol. 3, 356–467 (The Royal Society of Chemistry, 1976).
- Boudakian, M. M. Fluorinated Aromatic Compounds. *Kirk-Othmer Encyclopedia of Chemical Technology* <https://doi.org/10.1002/0471238961.0612211502152104.a01> (Wiley, 2000).
- Salonen, L. M., Ellermann, M. & Diederich, F. Aromatic rings in chemical and biological recognition: energetics and structures. *Angew. Chem. Int. Ed.* **50**, 4808–4842 (2011).
- Heidenhain, S. B. et al. Perfluorinated oligo(*p*-phenylene)s: efficient *n*-type semiconductors for organic light-emitting diodes. *J. Am. Chem. Soc.* **122**, 10240–10241 (2000).
- Sakamoto, Y. et al. Synthesis, characterization, and electron-transport property of perfluorinated phenylene dendrimers. *J. Am. Chem. Soc.* **122**, 1832–1833 (2000).
- Komatsu, S., Sakamoto, Y., Suzuki, T. & Tokito, S. Perfluoro-1,3,5-tris(*p*-oligophenyl)benzenes: amorphous electron-transport materials with high-glass-transition temperature and high electron mobility. *J. Solid State Chem.* **168**, 470–473 (2002).
- Sakamoto, Y. et al. Perfluoropentacene: high-performance *p*–*n* junctions and complementary circuits with pentacene. *J. Am. Chem. Soc.* **126**, 8138–8140 (2004).
- Nishida, M., Hayakawa, Y. & Ono, T. Formation of perfluorinated polyphenylenes by multiple pentafluorophenylation using C₆F₅Si(CH₃)₃. *J. Fluor. Chem.* **131**, 1314–1321 (2010).
- Troyanov, S. I. & Kemnitz, E. Synthesis and structure of halogenated fullerenes. *Curr. Org. Chem.* **16**, 1060–1078 (2012).
- Sakamoto, Y. & Suzuki, T. Perfluorinated and half-fluorinated rubrenes: synthesis and crystal packing arrangements. *J. Org. Chem.* **82**, 8111–8116 (2017).
- Lewis, S. E. Cycloparaphenylenes and related nano-hoops. *Chem. Soc. Rev.* **44**, 2221–2304 (2015).
- Segawa, Y., Yagi, A., Matsui, K. & Itami, K. Design and synthesis of carbon nanotube segments. *Angew. Chem. Int. Ed.* **55**, 5136–5158 (2016).
- Mirzaei, S., Castro, E. & Hernández Sánchez, R. Conjugated molecular nanotubes. *Chem. Eur. J.* **27**, 8642–8655 (2021).
- Rio, J., Erbahar, D., Rayson, M., Briddon, P. & Ewels, C. P. Cyclo-tetrahalo-*p*-phenylenes: simulations of halogen substituted cycloparaphenylenes and their interaction with C₆₀. *Phys. Chem. Chem. Phys.* **18**, 23257–23263 (2016).
- Jasti, R., Bhattacharjee, J., Neaton, J. B. & Bertozzi, C. R. Synthesis, characterization, and theory of [9]-, [12]-, and [18]Cycloparaphenylene: carbon nanohoop structures. *J. Am. Chem. Soc.* **130**, 17646–17647 (2008).
- Takaba, H., Omachi, H., Yamamoto, Y., Bouffard, J. & Itami, K. Selective synthesis of [12]cycloparaphenylene. *Angew. Chem. Int. Ed.* **48**, 6112–6116 (2009).
- Yamago, S., Watanabe, Y. & Iwamoto, T. Synthesis of [8]cycloparaphenylene from a square-shaped tetranuclear platinum complex. *Angew. Chem. Int. Ed.* **49**, 757–759 (2010).
- Myśliwiec, D., Kondratowicz, M., Lis, T., Chmielewski, P. J. & Stepień, M. Highly strained nonclassical nanotube end-caps. A single-step solution synthesis from strain-free, non-macrocyclic precursors. *J. Am. Chem. Soc.* **137**, 1643–1649 (2015).
- Tsuchido, Y., Abe, R., Ide, T. & Osakada, K. A macrocyclic gold(I)–biphenylene complex: triangular molecular structure with twisted Au₂(diphosphine) corners and reductive elimination of [6] cycloparaphenylene. *Angew. Chem. Int. Ed.* **59**, 22928–22932 (2020).
- Hashimoto, S. et al. Synthesis and physical properties of polyfluorinated cycloparaphenylenes. *Org. Lett.* **20**, 5973–5976 (2018).
- Leonhardt, E. J. et al. A bottom-up approach to solution-processed, atomically precise graphitic cylinders on graphite. *Nano Lett.* **18**, 7991–7997 (2018).
- Van Raden, J. M. et al. Precision nanotube mimics via self-assembly of programmed carbon nanohoops. *J. Org. Chem.* **85**, 129–141 (2020).
- Yamamoto, T., Abla, M. & Murakami, Y. Promotion of reductive elimination reaction of diorgano(2,2'-bipyridyl)nickel(II) complexes by electron-accepting aromatic compounds, lewis acids, and bronsted acids. *Bull. Chem. Soc. Jpn.* **75**, 1997–2009 (2002).
- Yamamoto, T., Murakami, Y. & Abla, M. Control of reductive elimination and acidolysis of diarylnickel(II) complexes by the kind of bronsted acid and the presence of oxygen. *Chem. Lett.* **28**, 419–420 (1999).
- Xia, J., Bacon, J. W. & Jasti, R. Gram-scale synthesis and crystal structures of [8]- and [10]CPP, and the solid-state structure of C₆₀@[10]CPP. *Chem. Sci.* **3**, 3018–3021 (2012).
- Segawa, Y. et al. Concise synthesis and crystal structure of [12] cycloparaphenylene. *Angew. Chem. Int. Ed.* **50**, 3244–3248 (2011).
- Segawa, Y. et al. Combined experimental and theoretical studies on the photophysical properties of cycloparaphenylenes. *Org. Biomol. Chem.* **10**, 5979–5984 (2012).
- Rio, J., Erbahar, D., Rayson, M., Briddon, P. & Ewels, C. P. Cyclo-tetrahalo-*p*-phenylenes: simulations of halogen substituted cycloparaphenylenes and their interaction with C₆₀. *Phys. Chem. Chem. Phys.* **18**, 23257–23263 (2016).
- Stasyuk, O. A., Stasyuk, A. J., Solà, M. & Voituyk, A. A. The hunter falls prey: photoinduced oxidation of C₆₀ in inclusion complex with perfluorocycloparaphenylene. *ChemPhysChem* <https://doi.org/10.1002/cphc.202200226> (2022).
- Nakanishi, Y. et al. Size-selective complexation and extraction of endohedral metallofullerenes with cycloparaphenylene. *Angew. Chem. Int. Ed.* **53**, 3102–3106 (2014).

37. Fujitsuka, M., Cho, D. W., Iwamoto, T., Yamago, S. & Majima, T. Size-dependent fluorescence properties of $[n]$ Cycloparaphenylenes ($n = 8\text{--}13$), hoop-shaped π -conjugated molecules. *Phys. Chem. Chem. Phys.* **14**, 14585–14588 (2012).
38. Segawa, Y., Levine, D. R. & Itami, K. Topologically unique molecular nanocarbons. *Acc. Chem. Res.* **52**, 2760–2767 (2019).

Acknowledgements

This work was supported by the ERATO program from the JST (JPMJER1302 to K.I.), the Funding Program for KAKENHI from MEXT (JP1905463 to K.I.; JP19H02701 and JP19K22183 to Y.S.), a grant-in-aid for Scientific Research on Innovative Areas “ π -Figuration” from the JSPS (JP17H05149 to Y.S.), the Toyoaki Scholarship Foundation (to Y.S.), the Daiko Foundation (to Y.S.), and the Mitsubishi Foundation (to Y.S.). Yuhei Miyauchi and JST CREST grants JPMJCR16F3 and JPMJCR18I5 are acknowledged for the support of photophysical measurements. The authors thank Shigehiro Yamaguchi, Soichiro Ogi, Masato Ito, Yoichi Kobayashi, Midori Akiyama, Yutaka Maeda, Iain A. Stepek, Yoko Shirota, Tsugunori Watanabe, Junya Shirasaki, and Hamamatsu Photonics K.K. for experimental support and fruitful discussions. T.K. is the recipient of a JSPS fellowship for young scientists (SPD). H.S. thanks the Nagoya University Interdisciplinary Frontier Fellowship and the Graduate Program of Transformative Chem-Bio Research (WISE Program) supported by MEXT. Computations were performed at the Research Center for Computational Science, Okazaki, Japan (22-IMS-C192). ITbM is supported by the World Premier International Research Center Initiative (WPI), Japan.

Author contributions

K.I. and Y.S. conceived the concept and prepared the manuscript with feedback from the other authors. H.S., M.K., and T.K. performed the synthetic experiments. Y.S. and H.S. performed the X-ray crystallographic measurements. M.S., T.N., and Y.T. performed the photophysical measurements. N.M. performed the Raman measurement. A.Y. provided critical comments.

Competing interests

The authors declare no competing interests.

Additional information

Supplementary information The online version contains supplementary material available at <https://doi.org/10.1038/s41467-022-31530-x>.

Correspondence and requests for materials should be addressed to Yasutomo Segawa or Kenichiro Itami.

Peer review information *Nature Communications* thanks the anonymous reviewer(s) for their contribution to the peer review of this work.

Reprints and permission information is available at <http://www.nature.com/reprints>

Publisher's note Springer Nature remains neutral with regard to jurisdictional claims in published maps and institutional affiliations.



Open Access This article is licensed under a Creative Commons Attribution 4.0 International License, which permits use, sharing, adaptation, distribution and reproduction in any medium or format, as long as you give appropriate credit to the original author(s) and the source, provide a link to the Creative Commons license, and indicate if changes were made. The images or other third party material in this article are included in the article's Creative Commons license, unless indicated otherwise in a credit line to the material. If material is not included in the article's Creative Commons license and your intended use is not permitted by statutory regulation or exceeds the permitted use, you will need to obtain permission directly from the copyright holder. To view a copy of this license, visit <http://creativecommons.org/licenses/by/4.0/>.

© The Author(s) 2022